

## **SINTERED SHEETS WITH HIGH POROSITY. STRUCTURE, PROPERTIES, PROCESSING**

**IOAN VIDA–SIMITI<sup>1</sup>**

*Abstract.* The paper represents a review of the research of the author related to sintered porous materials. It presents in a synthetic way the classification, the main properties and the functional characteristics of the porous sintered sheets: behaviour to mechanical stress, permeability and technological possibilities of processing. The sintered materials with high porosity can be mainly obtained from metallic and ceramic powders by free spreading methods followed by sintering. These types of materials have a structure characterized by porosity and a largely specific surface. The porous sintered structure consists of the framework of the basic metals (metallic matrix) and the spatial network of the pores. The metallic matrix made up of the sintered powder particle assures the resistance structure to the outside mechanical stress. The network of intercommunicating pores assures special properties and function to these types of materials, owing to porosity and highly specific surface. We can mention some of them: the filtering or cleaning of the fluids (gases and liquids) from impurities, the flame traps, sound absorbents, the fluidizing and uniform distribution of fluid on a surface or into a given volume, the separation of liquids or gases, the homogenizing (mixing) of a liquid with gas, catalytic and electrochemical properties, biotechnological properties.

*Key words:* sintered materials, porosity, porous materials

### **1. INTRODUCTION**

The porous materials obtained in layers by spreading or low compaction pressure by sintering metallic and ceramic powders represent porous materials with high porosity. They are used as a semi product to obtain some filtering elements of different geometric forms through procedures of plastic deformation, welding and machining. A classification of the porous materials with porosity and high specific surface according to the porosity and size pore is presented in figure 1 [1]. In figure 2 is shown a diagram of the technological itinerary for the manufacturing process sintered sheets with high porosity.

---

<sup>1</sup> *Professor, Ph.D. Eng, Technical University of Cluj-Napoca, [Vida.Simiti@stm.utcluj.ro](mailto:Vida.Simiti@stm.utcluj.ro)*

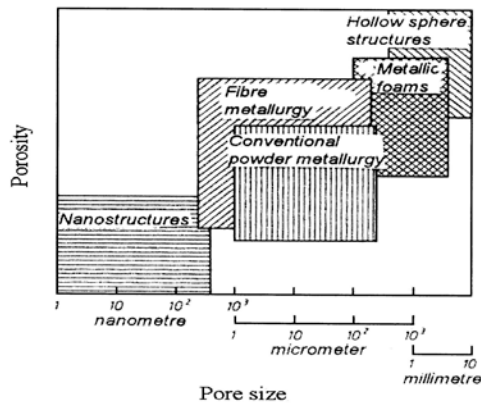


**Fig. 1. -** The classification of porous materials

some executing technological operations and exploitation.

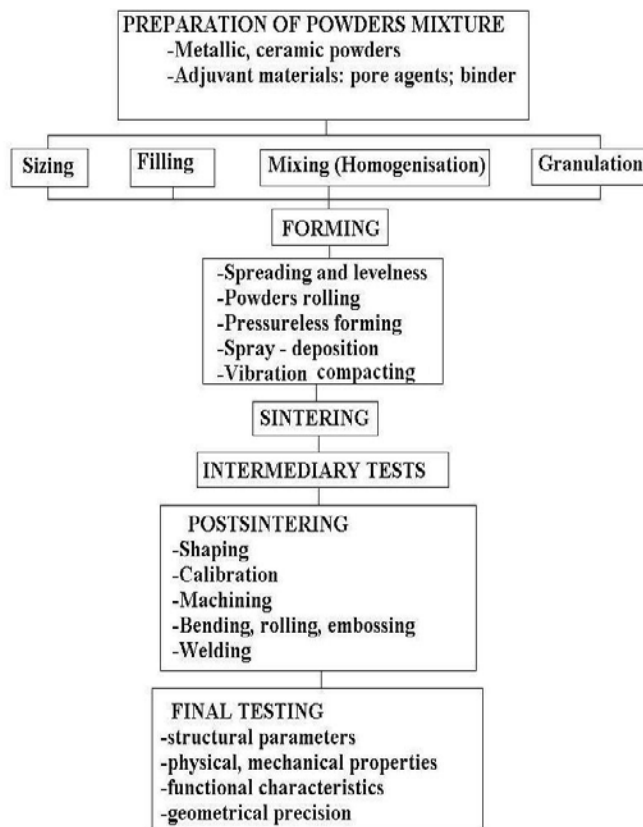


**Fig. 2. -**The diagram of technological itinerary for manufacturing the sintered sheets with high porosity]

The specific structure of these materials consists of a metallic frame formed of the grains of sintered powder and a spatial lattice of pores, most of them opened and intercommunicating with one another (Fig.3).

Intercommunicating pores ensure a good permeability of these materials [2, 3]. Sintered sheets of a very high porosity seem to be a new type of material with specific characteristics.

The sintered porous stainless sheets are subjected, among others, to tensile and compressive stresses during

These stresses have as an effect, modifications of the porous structure parameters followed by modifications of the main characteristics (filtering, technological and mechanical properties). Consequently, the study of sintered porous stainless sheets at compression and tensile stresses is necessary for an optimum dimensioning of filters and for determining the technological parameters to obtain different constructive forms [1,3]. The powder used to obtain the studied porous sheets by sintering is of the type 316 L (Höganäs). Its chemical composition consists of 0.3% C, 16...18% Cr, 10...12% Ni and Mo, 1% Si, 0.03% S, 0.03% P, the remainder being Fe.

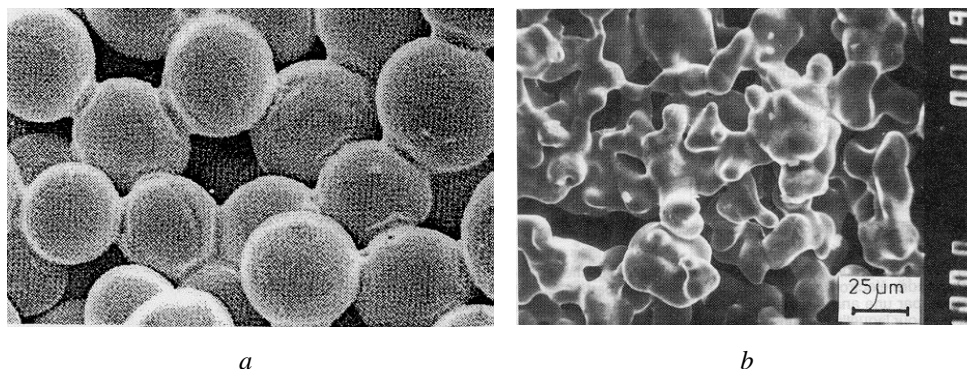


Fig. 3. - Porous sintered structures. a – spherical particles, b – irregular particles

## 2. MECHANICAL STRESS BEHAVIOUR

The homogenized powder is strewn with a strewing device on a steel sheet-metal used as a support. In view of the strewing operation, the support plates are isolated on both sides by covering them with a fine-grained slurry layer of  $\text{Al}_2\text{O}_3$ . The powder layer is then dressed at the desired thickness (1...2 mm). The tests presented in the paper have been performed on sintered porous sheets of 1.5 mm thickness.

Sintering has been performed in a protective atmosphere of hydrogen. The influence of sintering parameters on the optimum porous structure of desired porosities has been studied. For the particle size range used in the work ( $-40\ \mu\text{m}$ ;  $+40\text{-}80\ \mu\text{m}$ ;  $+80\text{-}125\ \mu\text{m}$ ), the temperature range within (1290...1310) °C (at sintering time 120 min) has permitted to obtain certain sintered sheet-metals having an optimum porous structure and the porosities given in the paper [4,5].

### 2.1. Tensile Test

To determine the mechanical characteristics (the tensile strength, the conventional yield limit, the elongation on fracture), tensile tests on a large number of samples cut from porous sheets of different porosities and of different initial-particle size range have been made on a universal testing machine of the “Instron” type.

For the tensile testing of porous sheets, a new type of sample with the shape and dimensions presented in Fig. 4, being manufactured by applying highly accurate cutting in order to raise the dimensional

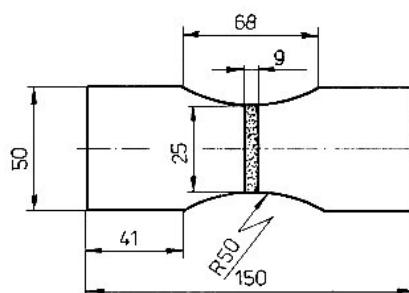


Fig. 4. - Specimen used for tensile test

accuracy and to diminish the failings from the cutting zone, has been used. The shape of the circular arc (R 50), adopted for the gauged zone of the sample, imposes the fracture of each sample in the central part, namely at the minimum width of 25 mm [4].

In the case of tensile strength as a function of porosity, considering (for this study) each particle size fraction separately, the dependence relations with the least values of the residuum of the mean residuum and of Gaussian concordance test, are those of the experimental type. Thus, the variation law of tensile strength as a function of porosity is the relation [4, 5, 6]:

$$R_p = R_m \cdot \exp(-V_1 P) \quad (1)$$

where:  $R_m$  – the tensile strength of the matrix of material compact powder;  $P$  – Porosity;  $V_1 = 5.13$  for the particle size  $-40 \mu\text{m}$ ;  $V_1 = 5.86$  for the particle size  $(+40-80) \mu\text{m}$ ;  $V_1 = 6.63$  for the particle size  $(+80-125) \mu\text{m}$ .

The parameter  $V_1$  represents the decreasing rate of the tensile strength with increasing porosity. From the data given above, one can see that  $V_1$  increases linearly with the increasing size range of the powder used. Therefore the tensile strength of the sheet decreases.

With regard to the tensile strength, it is not unimportant whether the material porosity consists of many and small pores (the case of small size particles) or of few and big pores (the case of big size particles). In the latter case, the tensile strength will be less at the same porosity than it is in the first case.

If the size powder range used is left aside and all the experimental results are taken into account for the whole porosity range, the dependence of the tensile strength on the porosity is more complicated, being described as a relation of type:

$$R_p = R_m (1 - P^2)^2 \cdot \exp(-V_2 P) \quad (2)$$

where:  $V_2 = 4.49$ .

In case of yield limit variation of the sintered porous stainless sheets as a function of porosity, the variation law that may be used in all cases, regardless of powder size range, is a law of type (2) with  $V_2 = 2 \dots 5$ , depending on the powder size range [4, 5, 6]:

$V_2 = 2.27$  for the particle size  $-40 \mu\text{m}$ ;

$V_2 = 3.48$  for the particle size  $(+40-80) \mu\text{m}$ ;

$V_2 = 4.39$  for the particle size  $(+80-125) \mu\text{m}$ ;

$V_2 = 3.12$  regardless of the particle size.

The curves 4 in Figs. 5 and 6 show the same dependencies when the powder size used is left aside. These curves have only been included for comparison with curves 1, 2, 3, which were experimentally determined and plotted by the computer for each powder size range used to obtain the porous sheets under consideration.

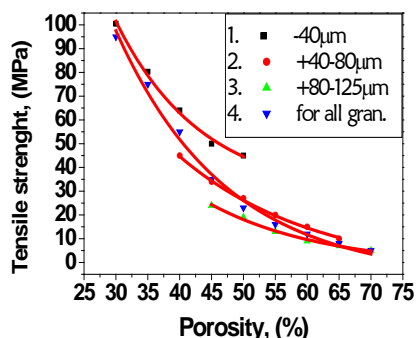


Fig. 5. - Dependence of tensile strength on porosity and particle size range

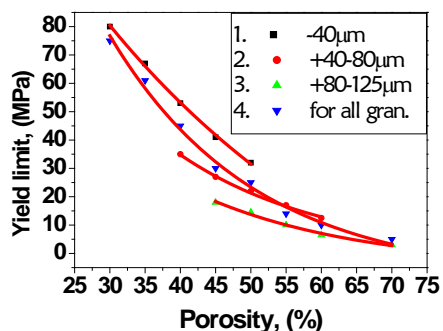


Fig.6. Dependence of yield point on porosity and particle size range

The curves obtained in this way may be used to determine the tensile strength and yield limit of a sintered porous stainless sheet of high porosity.

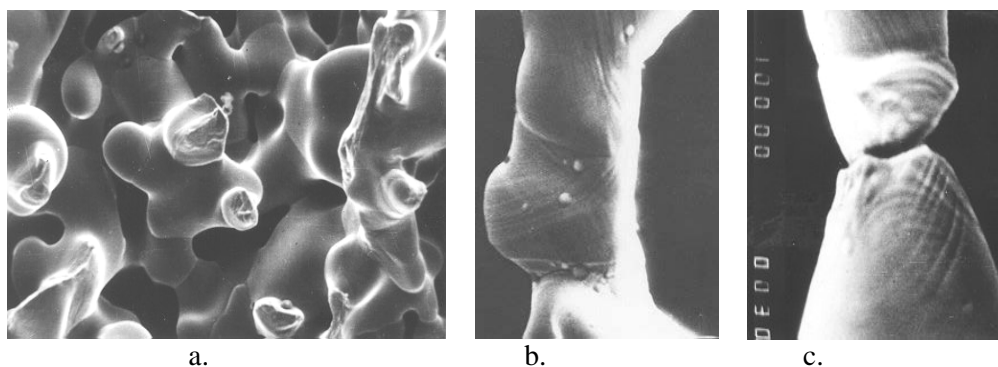


Fig. 7. - SEM images of the fracture: a - general view (x1000), b – elongated sintering neck (x10000), c - fractured neck (x10000)

The analysis by scanning electron microscopy of the fracture surfaces of the porous sheet samples subjected to traction underline the fact that the fracture zone is localized in the sintering necks generated through sintering (fig.7) [4]. These necks represent some nick zones that are real concentration zones of the tensions that govern the way of fracture as well as the propagation mechanism of the cracks. With the experiments performed on porous materials of austenitic stainless steel powders, the majority of the fractures have taken place after well-marked plastic deformations of the sintering neck with a large radius of curvature. This fact denotes the reduced or inexistent effect of the tensional concentration in the zone of most of these necks. In Fig.7c, even the presence of the sliding planes was noticed on some fractured necks. This justifies the moderately ductile character of the necks fracture, due to the

austenitic structure of the metallic matrix. But, on the porous material assembly, the fracture of the porous metals may be considered as having a brittle character.

## 2.2. Compression Test

The hydrostatic pressure of the fluids that are filtered as well as the mechanical action of some metallic parts that are in contact with the porous body, cause its deformations, a fact that justifies the necessity of the compression test of thin porous sheets.

Compression testes on samples of sintered porous stainless sheets of different initial thicknesses and porosities with a punch of 11.3 mm in diameter were carried out on a machine of the Instron type. During each loading step, the load (as well as the respective pressure) has been calculated with the equation:

$$\varepsilon = \ln \frac{h_0}{h} \quad (3)$$

The porosity obtained after each deformation step been determined. The experimental results suggest the following relations for characterizing the dependence:

$$p = A \cdot \exp(B \cdot \varepsilon) \quad (4)$$

$$P = P_0 \cdot \exp(C \cdot p) \quad (5)$$

$$P = 1 - (1 - P_0) \cdot \exp(M \cdot \varepsilon) \quad (6)$$

where  $p$  is the deformation pressure;  $\varepsilon$  the monoaxial plastic deformation;  $P$  the current porosity;  $P_0$  the initial porosity;  $A$ ,  $B$ ,  $C$ ,  $M$  are parameters.

In Figs. 8, 9 and 10, the form the characteristics  $p=f(\varepsilon)$ ,  $P=f(p)$ , and  $P=f(\varepsilon)$  is presented in case of compression, described by relations – with the  $A$ ,  $B$ ,  $C$  and  $M$  parameters determined on the computer.

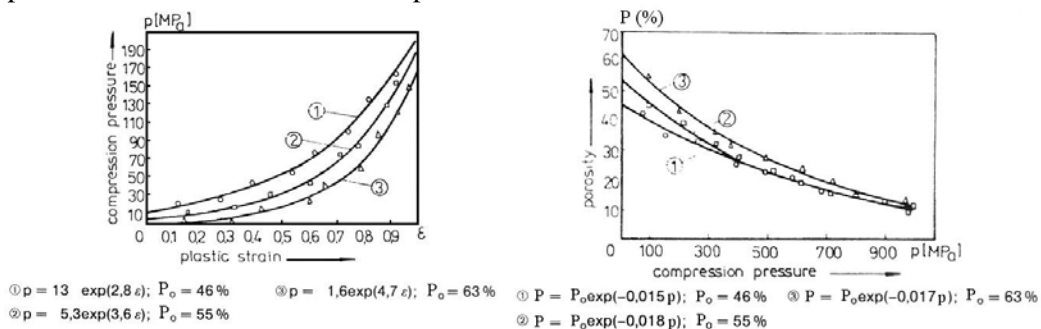


Fig. 8. - Compression strain curves

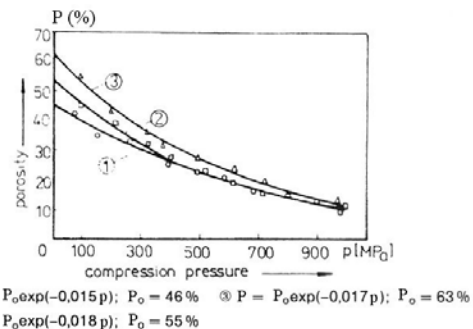
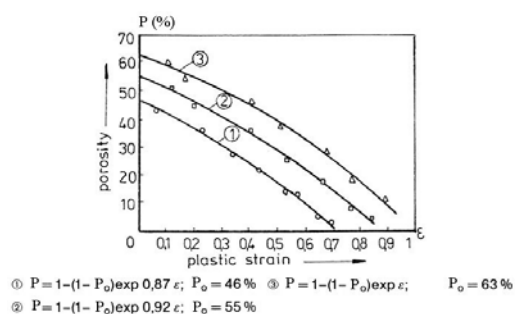
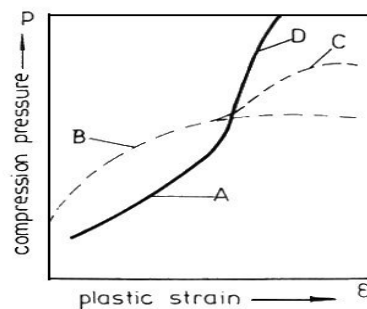


Fig. 9. - Porosity variation depending on pressure



**Fig. 10.** - Porosity variation depending on strain



**Fig. 11.** - Characteristic shapes of strain curves: A+D – porous sintered sheet; B – compact material; C – sintered material with reduced porosity

As can be seen from these figures, the values of these parameters are in close agreement with the theoretical considerations concerning the initial porosity dependence  $P_0$  of the compression behaviour of sintered stainless sheets of high porosity.

The compression deformation characteristics of the sintered porous sheets of high porosity (Curve A) are different from those of the compact materials and of the sintered materials of a low initial porosity (Curve B in Fig. 11). This shape variation of the curves may be explained by the decrease of the material porosity at compression.

When the complete compaction is achieved by compression, theoretically the material tends to behave like compact materials (Curve C). But a well-marked increase of the pressure is noticed, together with small deformation increases (Curve D) till the complete crushing of the material under the punch takes place. The disagreement in shape between the curves C and D may be explained by a well-marked strain hardness of the metallic matrix material, at the same time with the deformation and compaction in the zone of Curve A.

### 3. INFLUENCE OF THE TECHNOLOGICAL PARAMETERS ON THE STRUCTURE AND PERMEABILITY

From the powders classified into four powder size range, porous samples were realized by spreading, pressing and sintering in the shape of disk tablets with 60 mm diameter and about 3 mm thickness. The powder size range, the formation procedure, compacting pressure and sintering regime influences the porous structure's porosity and pores sizes. For the current studies five powder size range of stainless steel powder (316L) was used.

In order to determine the maximal size of pores, the bubble test was used according to the methodology provided by the international standard EN 24003.

Figure 12a presents the influence of the compacting pressure on the porosity for all the size range of the stainless steel powders used. As expected, a marked

decrease of porosity was found, following the compacting pressure and the reduction of the size of the particles. The porosity as a structural parameter may be considered as a guiding influence factor on some filtrating functional characteristics of permeable porous structures: the permeability and filtering fineness.

Figure 12b presents the influence exerted by the compacting pressure as a technological factor on the pore size and on the maximal size respectively for each particle size range of the stainless steel powder used. The maximal size of the pores increases from one size range to the other in parallel with the increase of the powder particles. This tendency is explained by the different size of the empty spaces left in the arrangement of the compacted particles. Therefore the particle size range fraction represents a determinant factor of the permeable porous structure and its parameters.

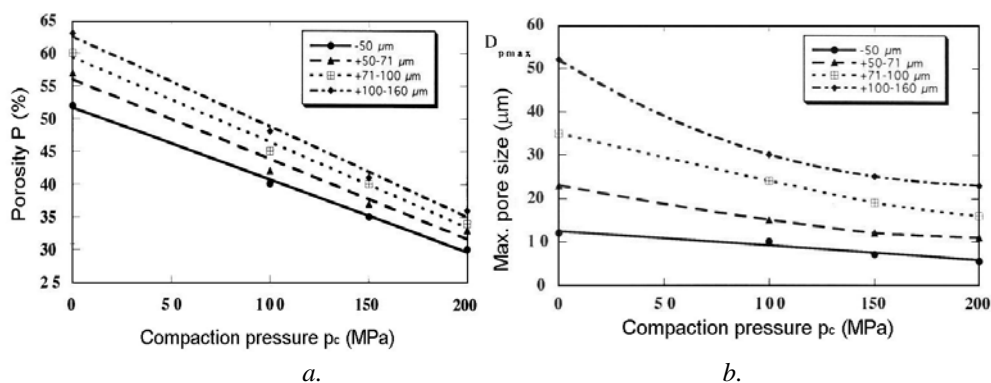


Fig. 12. - Influence of compacting pressure on porosity (a) and pore size (b)

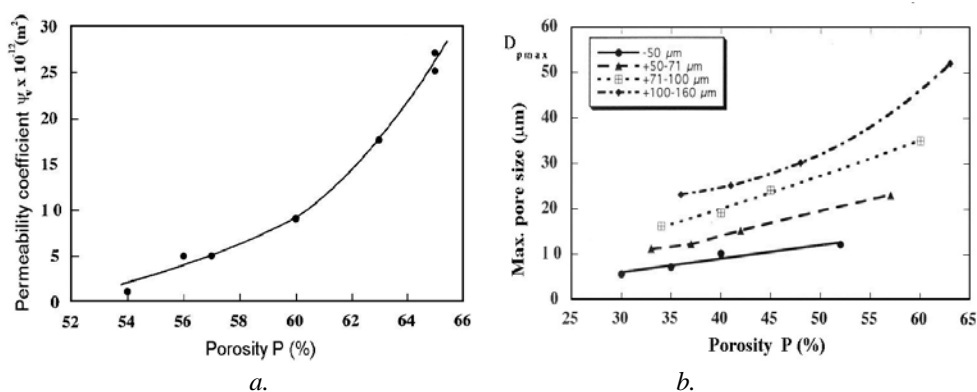


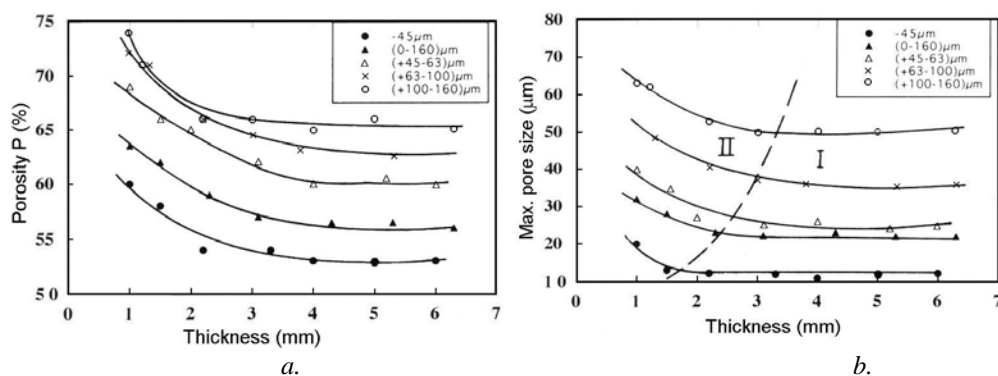
Fig. 13. - Variation of the permeability coefficient (a) and maximal pore size (b) according to porosity

Figure 13 presents the influence of the porosity on the viscous permeability coefficient (a) and the maximal pore size (b) in the case of air flow through the pores.

The change of porosity resulted in the increase of the compacting pressure and powder size range.

#### 4. "SURFACE EFFECT" IN THE POROUS SINTERED SHEETS

In the case of thin sintered sheets obtained from powders, there are variations in same structural and functional parameters depending on thickness. From a certain thickness, depending on the powder size, there is a uniformity of the porous structure which ensures the reproducibility of the parameters and functional characteristics [6, 7].



**Fig. 14.** - Variation of porosity (a) and maximal pore size (b) with the thickness of the porous sheet

The papers presents the results of experimental researches concerning the influence of the thickness of permeable sintered layers from stainless steel powders with different particle size on some structural and functional characteristics: porosity, pore size.

For each powder size range used for the experiments, the porosities and the maximal pore dimension of the obtained sheets are higher at the minimal thickness, decreasing up to certain values which subsequently remain constant (Fig.14).

As the superficial layers of the sheets have reduced densities, and consequently higher porosities compared to the rest of the porous body, the "surface effect" manifests its influence in the case of thin sheets. Thus, the lower porosity of the superficial layers influences the porosity value of the porous body as a whole, reducing its effect or disappearing completely at higher thickness. The effect is more marked in the case of sheets obtained from greater and larger powder particle sizes. From a certain thickness the surface effect loses its influence.

The critical thickness and the maximal equilibrium size (equalling dimension) of the pores  $D_{p_{max,e}}$  for each powder size range are shown in table 1.

**Table 1. Values of critical thickness and equalling dimension**

Size range	-45 [ $\mu\text{m}$ ]	0+160 [ $\mu\text{m}$ ]	+45-63 [ $\mu\text{m}$ ]	+63-100 [ $\mu\text{m}$ ]	+100-160 [ $\mu\text{m}$ ]
g [mm]	1.5	2	2.5	2.8	3.0
$D_{p \text{ max.e}}$ [ $\mu\text{m}$ ]	12.3	22	25	36	50

The higher values of the maximal pore dimension for thickness less than the critical ones are also due to the “surface effect”, which also manifests in this case due to the imperfect arrangement of the powder particles that diminish the ordering degree of the structure. At greater thickness there are more powder layers by which the particle arrangement is stabilized, the porous structure tending to become regular.

Zone I (Fig. 14) determined by the higher values of the critical thickness, corresponds to the ordered, regular porous structures, and zone II to the irregular structures, with reproducible structural parameters and functional characteristics.

## 5. TECHNOLOGICAL PROCESSING POSSIBILITIES OF SINTERED SHEETS

### 5.1. Bending

One of the procedures of plastic deformation by which tubular parts can be made of sintered porous sheets is rolling. The principle of rolling is the wrapping of the porous sheet over a central cylindrical roller having a diameter equal to that of the tube to be executed by using another roller with smaller diameter (Fig.15).

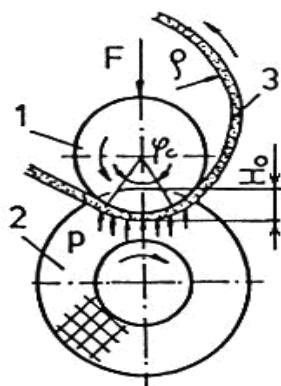


**Fig. 15.** - The diagram of the rolling with elastic cylinder of sintered porous sheets

The presence of compression forces determines an increase of the deformation capacity of the materials, namely smaller values of the minimal rolling radius as compared to the bending ones.

Another method providing a high curving capacity for sintered porous sheets is bending (rolling) with elastic cylinder [8,9,10]. This procedure also has the advantage of protecting the porous structure by reducing or excluding the crushing effect at the contact under pressure of the sheet with the active elements of the bending device.

Bending with elastic cylinder (fig. 16) is a forming and modelling process, by rotation, of rolling type, where one of the cylinders is rigid, the other one being covered by a layer of elastic material (polyurethane). The two cylinders, as rolling active elements, have unequal diameters. On the contact surface, along the angle of contact  $\rho_c$ , between the porous sheet (3) and the elastic layer (2) there appears a uniformly distributed load, due to the pressing force action of the rigid cylinder. The rotating movement provides a successive forming and modelling, the sheet coming out of the

contact zone with a curvature depending on the pressing force, respectively on the depth of penetration in the elastic layer [8].

The tested sheet was obtained by sintering the layers made of austenitic stainless powder (316 L), freely spread and smoothed at the above thicknesses, having a particle size range of (0...160) $\mu\text{m}$  and a porosity after sintering of approximately 45%.

Figure 16 presents the influence of pressing force (a) and penetration (b) on the curvature relative radius. When increasing the pressing force, a growth of the curvature, respectively a diminution of the bending relative radius is noted. This variation is explained by the greater contact angle between the roller 1 and the porous sheet when increasing the pressing force, so the forming and modelling effect becomes stronger. The data in the diagram represent the arithmetic mean of the experimental results.

The dependence laws of the curvature relative radius versus the pressing force and the depth of penetration, which best describe the experimental results, are exponential type relations:

$$\rho_{rel} = A_1 \cdot \exp(-B_1 F) \tag{7}$$

$$\rho_{rel} = A_2 \cdot \exp(-B_2 H) \tag{8}$$

where:  $A_i, B_i$  are parameters determined by computer.

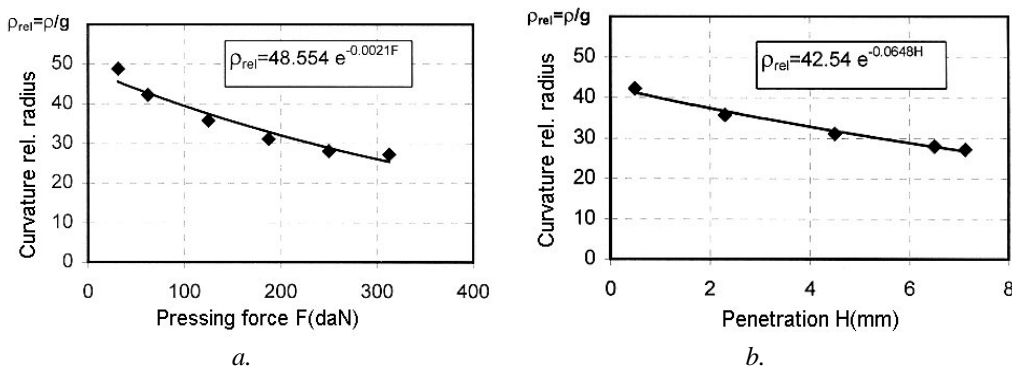


**Fig. 16.** - Influence of the pressing force (a) and penetration (b) upon on the curvature relative radius

The hyperbolic shape of the dependence law for compact sheets does not correspond in all respects in the case of sintered porous sheets.

As a result of crushing tests (pressure with a hob) of sintered porous sheets, with or without and intermediary elastic layer (polyurethane), the structural aspect is completely different. In the case of direct crushing (without intermediary elastic layer), the intense densification and pore bridging may be noticed, while with interposition of

an elastic layer between the hob and the material, this effect is reduced or inexistent at relatively low pressing forces.

## 5.2. Electrical Discharge Cutting using Wire Electrode

The specific porous structure of sintered sheets influences the process of cutting by electrical erosion using wire electrode [11]. The properties of sintered porous material and the specific conditions in which the erosion process by electrical electrode takes place develop the process of local melting and flow in the thermally influenced zone with the reduction of the initial porosity and also the size of pores. The productivity of wire electrical erosion cutting of porous sintered materials is expressed by the cutting speed increase with the porosity and the work intensity. The defects discovered in the thermally influenced zone are by far more reduced as compared to other methods of cutting-out (shearing, flame cutting, plasma cutting). The method of electrical discharge with wire electrode is recommended for the processing of porous sintered sheets in order to obtain parts of complex shapes with geometrical precision, high quality cutting surface and without substantial marginal defects (fig. 17 ).

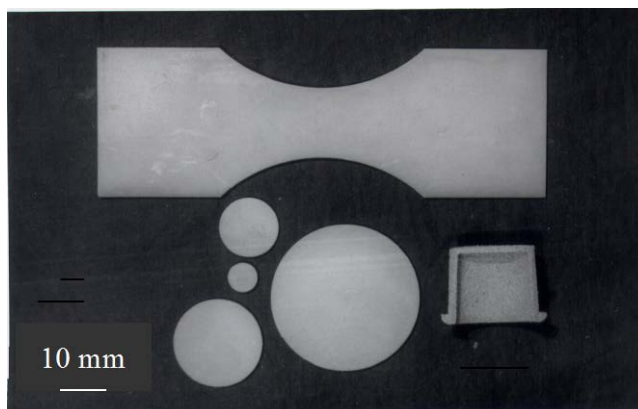


**Fig. 17.** Samples cut out by electrical erosion using wire electrode

Experimental tests were performed using sintered porous sheets obtained by free spreading of austenitic stainless steel powder type 316L, (1.75...2.00) mm thickness and porosity ranging between 15 and 40 %. The sintering conditions are: temperature 1300 °C and sintering time, 120 minutes. A type AGIECUT 250 devices for wire electrical discharge cutting with digital command was used in the following conditions of cutting-out technology: the dielectric - de-ionized water, wire copper electrode of 0.2 mm diameter; wire travelling speed 20 mm/s; discharge tension 150 V. After preliminary trials the optimal value of the condenser capacity in the discharge circuit was established at 150 nF, corresponding to a finishing regime [12]. At higher

values the almost complete closure of pores on the cut surface was found, therefore the influence was so strong that the affected zone was no longer porous.

Analyzing the area thermally influenced following the cutting process a number of effects on the porous structure were found.

The thermal effect was located in the cutting area, namely around the discharge craters, and its influence on the structure and depth of the superficial layer was correlated with the discharge energy.

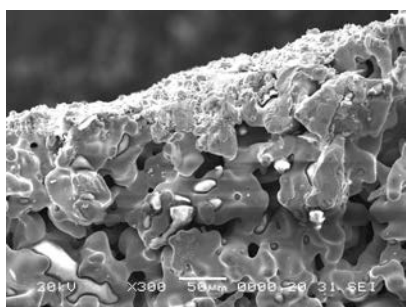


**Fig. 18.** - The thermally influenced area at electrical discharge cutting with wire electrode of the sintered porous sheet (SEM - 300X)

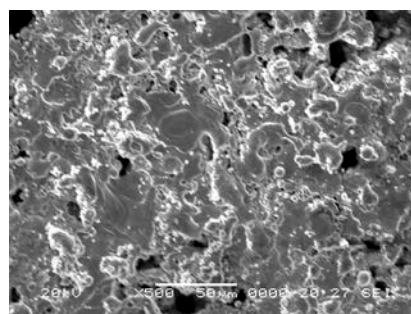


**Fig. 19.** - The aspect of the surface resulting by electrical discharge cutting with wire electrode (SEM - 500X)

Analysis of the SEM images of the thermally influenced layer in comparison with the initial porous structure evidenced distinct areas of lower porosity and with much smaller pores (fig.18). The high temperature due to the electrical discharge as well as the lower thermal conductivity of the porous material caused additional sintering by increasing the size of the interparticles necks, reduction of the size of pores and porosity. Both on the cut surface and the thermally influenced area partially melted and resolidified particles may be noted (fig.19). These processes developed in the areas of electrical discharge of micro channels of ionization of high temperature, whose sizes may be considered to be of the same order as the ones of the interparticles necks.

In conditions of local melting inherent to the process, other physical and chemical phenomena may occur that influence the micro- and macrostructure of the material. Thus, it is possible that a part of the melt material will evaporate, then condense and deposit, while another melt part will flow and by the capillarity effect penetrate into the pores of the cut surface or the neighbouring pores. It may be stated that the above-mentioned cumulative effects lead to the decrease of porosity and size of pores in the thermally influenced area.

The process of electric erosion is also accompanied by the superficial oxidation of the material exposed to erosion. The atomic oxygen resulted from the decomposition of ionized water will oxidize the component elements of the alloy (e.g., Fe, Si, Cr). The oxides formed appear in the form of fine pellets on the cut-out surface

It may be stated that the area thermally influenced following the process of wire electrical cutting of sintered porous materials is relatively small, while the extent of the margin defects evidenced (reduced porosity, pore closure, superficial oxidation) is not too great. The consequences of the presence of these defects are much more reduced as compared to the ones induced by the mechanical cutting procedures such as plastic deformation or shearing. In some cases it may be considered that the reduction of porosity is beneficial, the cut-out area representing the very joining area between the porous part and other mounting elements in the subunit of which it is a component.

Figure 20 presents the influence of porosity on the cut speed for different values of the current intensity. The cut speed is defined by the value of the cut section per time unit. A slight increase of the cut speed (assessed by the times to cut constant lengths of material) was found when porosity increased. This may be explained by the decrease of the actual section of the material of the cut metallic matrix at the same discharge capacity, namely the implicit increase of the travelling speed. Based on these results the dependence correlation between the cut speed and the current intensity may be calculated for each value of porosity (fig. 21). Increase of the current intensity will decrease the cut time, i.e. increase of the cut speed, following increased discharge energy and more intense erosion process.

However, both graphs evidence a more reduced influence of the porosity on the cut speed. Practically the curve slope is relatively small. The effect of re-sintering and re-penetration of the eroded material into the pores reduces the more marked influence of the initial porosity.

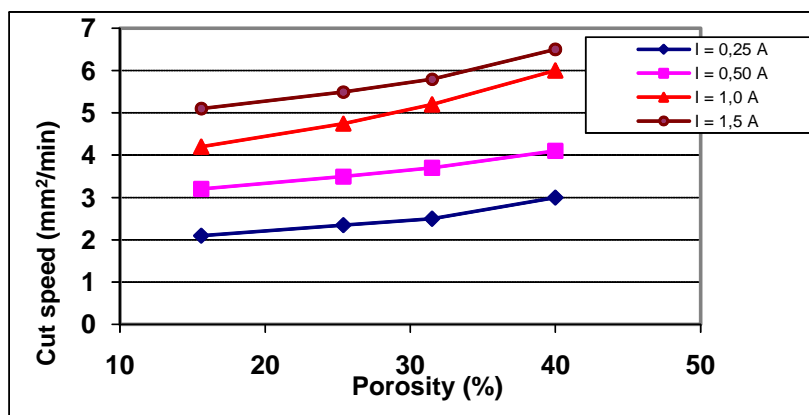


Fig. 20. - The influence of porosity on the productivity in the electrical discharge cutting

## 6. CONCLUSIONS

The dependence laws of the mechanical characteristics as a function of the sheet porosity of stainless metallic powder of high porosity are of an exponential form according to relations (1), (4)-(6).

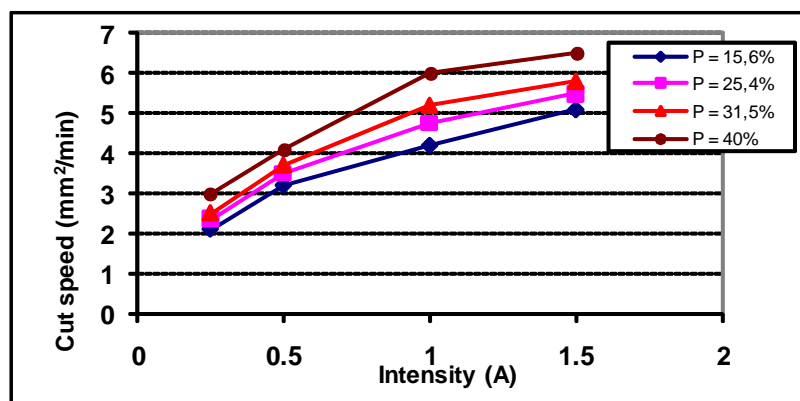


Fig. 21. - The dependence of the productivity on the current intensity in the electrical discharge cutting

- At the analysis of the mechanical characteristics as function of porosity, the particle size of the powder used must be considered.
- At the level of the sintering necks, the fracture of the sintered porous stainless materials has a ductile character.
- The compression deformation characteristics of the sintered porous sheets of high porosity have a different form from those of compact and sintered materials with reduced porosity.
- The process of bending by rolling of porous sintered sheets will observe the minimal bending radius in order to avoid fissuring of the exterior layer.
- The minimal rolling radius (deformability indices) depends on the thickness and porosity of the porous structure and represent and indicator of the deforming capacity.
- The current researches led to patenting the manufacturing of porous tubes by rolling the porous sintered sheets using cylindrical elastic tubes.
- For each particle size range fraction used there are porosity variations at reduced thickness of the porous samples, due to the “surface effect”.
- A critical thickness of the porous permeable layers is found, from which the maximal pore dimension remains constant, the uniformity coefficient has the value one, and so the porous structure becomes ordered, tending to regularity and reproducibility.
- The porous structure of sintered sheets influences the process of wire electrical discharge cutting.
- The properties of the sintered porous material (especially decreased thermal conductivity) and the conditions induced by the electrical discharge erosion (high temperatures) develop the re-sintering process in the thermally influenced area, with decrease of porosity, reduction of pores and their clogging by the eroded material.

- The cutting productivity of the wire electrical discharge procedure for sintered porous materials, expressed by the cut speed, increases with porosity and the intensity of the electrical current applied.
- Certain defects evidenced in the thermally influenced area (more dense porous structure, oxidation of chemical components) generate considerably more reduced adverse effects than in case of other methods of cutting metallic sheets. In most cases these defects have a positive influence on the assembling capacity of the sintered porous parts.
- The wire electrode electrical cutting of sintered porous sheets is recommended in order to obtain parts with complex shapes and high geometrical precision, high quality cut surface and tolerable marginal defects.
- The results obtained in the present study are necessary both for determining some functional parameters and for establishing the manufacturing technology of the permeable porous pieces (filters, flame traps, sound absorbers etc.).

#### REFERENCES

- [1]. **W. Schatt, K.P. Wieters** - *Powder Metallurgy. Processing and Materials*, EPMA, (1997).
- [2]. **Albano-Müller**, *Powder Metallurgy International*, **14**, p. 73-79, (1982).
- [3]. **G. A Wilson**, - *Porous Metal Filters. Selected Case Studies in PM, The Institute of Metals Series on PM*, London, p. 76-91, (1991).
- [4]. **A Palfalvi, I Vida-Simiti, I Chicinaş, L Szabo, I Magyorosi**, *Powder Metallurgy International*, **4**, p. 16-19, (1988).
- [5]. **I. Vida-Simiti**, *Journal of Optoelectronics and Advanced Materials*, **8**, p.1479-1483, (2006).
- [6]. **Keishi, Gotoh**, *Powder Technology*, **20**, p. 257-260, (1978).
- [7]. **R.P. Todorov**, *Poroskovaja Metallurgija*, **3**, p. 31-33, (1986).
- [8]. **I. M. Zakirov** - *Gibka na valkah s elastycznym pokrytyem*, Masinostroenie, Moskva, (1985).
- [9]. **I Vida-Simiti, V Seiculescu**, *Proceedings, Deformation and Fracture in Structural PM Materials*, Slovakia, 1996, (1), p. 318-323.
- [10]. **I. Vida-Simiti, C. Ciupan**, *Process for Making Porous Tubes by the Rolling with Elastic Layer of Sintered Sheet Metal*, Patent Number(s): RO123245-B1/2011 ; RO123245-B8
- [11]. **Z. Sparchez, I. Vida-Simiti**, *Proceedings, World Congress PM 2004*, Viena. p. 383-389.
- [12]. **I. Vida-Simiti, Z. Sparchez**, *Proceedings, World Congress on Powder Metallurgy*, PM 2004, Viena, 2004, p.359- 365.